Eur. Phys. J. D **16**, 145–149 (2001)

THE EUROPEAN PHYSICAL JOURNAL D

EDP Sciences

Vibrational wave packet dynamics in the silver tetramer probed by NeNePo femtosecond pump-probe spectroscopy

H. Hess[a], K.R. Asmis[b], T. Leisner[c], and L. Wöste

Institut für Experimentalphysik, Freie Universität Berlin, D-14195 Berlin, Germany

Received 30 November 2000

Abstract. We present results on the ultrafast dynamics of mass-selected neutral Ag_4 clusters using NeNePo (negative ion - neutral - positive ion) femtosecond pump-probe spectroscopy. One-color pump-probe spectra of the $Ag_4^-/Ag_4/Ag_4^+$ system measured at 385 nm and an internal cluster temperature of 20 K display a complex beat structure over more than 60 ps. The oscillatory structure is attributed to vibrational wave packet dynamics in an excited "dark" state of neutral Ag_4. A dominant 740 fs wave packet period as well as wave packet dephasing and rephasing are observed in the spectra. Fourier analysis of the spectra yields a group of frequencies centered around 45 cm^{-1} and an anharmonicity $|2\nu_0\chi_e|$ of 2.65 cm^{-1} for the active vibrational mode.

PACS. 36.40.-c Atomic and molecular clusters – 33.15.Mt Rotation, vibration, and vibration-rotation constants – 33.80.Eh Autoionization, photoionization, and photodetachment

1 Introduction

The development of ultrafast spectroscopic techniques has enabled scientists to probe dynamical processes in matter with unprecedented temporal resolution [1–3]. NeNePo (negative ion - neutral - positive ion) femtosecond pump-probe spectroscopy is a versatile tool to study nuclear dynamics on the potential energy surface (PES) of mass-selected, isolated neutral clusters and molecules in real time [4,5]. In comparison to femtosecond pump-probe experiments on (neutral) molecular beams three main advantages may be pointed out. (1) Mass selection prior to interaction with the laser field uniquely identifies the signal carrier even when highly fragmentative systems are investigated. (2) Photodetachment of the anion often allows to populate regions of the neutral PES by vertical transitions, which are not accessible by photoabsorption of the neutral species. (3) Due to the different selection rules for photodetachment of the anion compared to photoabsorption of the neutral species so-called "dark" states can be accessed.

NeNePo femtosecond pump-probe spectroscopy was pioneered by Wöste and coworkers, who studied the isomerization reaction from linear to cyclic Ag_3 in real time [4]. This experiment stimulated further experimental [5–8] and theoretical efforts [9–12], which allowed for a detailed description of the rearrangement process on the ground state PES of the silver trimer. Experimental and theoretical efforts were then extended to larger silver clusters [13–15]. Yannouleas and Landman predicted that the NeNePo scheme should be useful to characterize low frequency vibrations in Ag_{14}, manifested by coherent revivals in the $Ag_{14}{}^+$ signal [15]. However, no recurrences were observed in the experiments on Ag_3 and larger uneven numbered silver clusters. In Ag_3 this was attributed to resonant intramolecular vibrational energy distribution (IVR) taking place on a time scale of a few ps, *i.e.*, on a similar time scale as the turnaround time of the vibrational wave packet [12]. For larger metal clusters IVR is expected to be even faster, due to the increase of the degrees of freedom with cluster size. The question thus arises, if NeNePo femtosecond pump-probe spectroscopy can be used to monitor nuclear dynamics in larger metal clusters or if energy dissipative effects result in a too rapid dephasing of the wave packet motion and thus mask its spectral signature?

In the present study we present the NeNePo spectra of the $Ag_4^-/Ag_4/Ag_4^+$ system. The energetics of this system have been studied in some detail both experimentally and theoretically. The 351 nm anion photoelectron spectrum of Ag_4^- reveals three peaks at binding energies of 1.65 eV, 2.39 eV, and 2.76 eV assigned to the ^1A_g ground state and $^3B_{1g}$ and $^1B_{1g}$ excited states of neutral Ag_4 with rhombic geometry (D_{2h}) [16–20]. Fluorescence and excitation spectra of Ag_4 deposited in an argon matrix as well as anion photoelectron spectra recorded at higher photon energies reveal additional excited states of Ag_4 at

[a] *Present address:* Department of Bioengineering, University of Washington, Seattle WA 98195, USA.

[b] e-mail: asmis@physik.fu-berlin.de

[c] *Present address:* Institut für Experimentalphysik II / Umweltphysik, Technische Universität Illmenau, D-98684 Illmenau, Germany.

higher energies [21,22]. An ionization energy of 6.65 eV for Ag_4 has been deduced from electron impact ionization measurements [23]. Theoretical calculations predict rhombic D_{2h} ground state geometries for all investigated three charge states [24–28].

The present study is a continuation of our efforts on studying the dynamics and reactivity of noble metal clusters, which have received considerable attention, *e.g.*, due to the important role these clusters play in catalytic and photographic processes [29,30]. The paper is structured as follows. After a brief description of the experimental apparatus, we present the results of real time measurements of the $Ag_4^-/Ag_4/Ag_4^+$ system combined with an interpretation and discussion of the data. We conclude with an outlook on future experiments.

2 Experimental methods

The pump-probe experiments were performed in a modified guided ion beam apparatus using ultra-short laser pulses from a regeneratively amplified femtosecond laser system. Both have been described previously, and only the salient features will be summarized [7,8].

The ultrashort laser pulses are generated by a Nd:YLF laser-pumped regenerative amplifier (Quantronix 4800), seeded by a titanium-sapphire oscillator (Spectra Physics Tsunami) which is pumped by a Nd:YAG laser (Spectra Physics Millennia V). After an additional multi-pass amplifier tunable pulses in the wavelength range from 765 nm to 845 nm with energies of up to 1.6 mJ at a repetition rate of 1 kHz are generated. The light is frequency doubled in a 0.5 mm thick BBO crystal, resulting in band-width limited pulses with a duration of 130 fs. The laser beam is then divided by a beam splitter. One beam passes through a computer-controlled delay stage and is recombined with the other beam. Before being introduced collinearly with the quadrupole arrangement through the detector flange of the quadrupole system both beams are focused with a 100 cm lens into the center of the ion trap.

Silver clusters are generated in a modified cold reflex discharge ion source (CORDIS). Negatively charged clusters are guided into a He-filled quadrupole ion guide, which collimates the ion beam and cools the initially hot ions to room temperature. Subsequently, the cluster ions of interest are mass-selected by a quadrupole mass filter. Mass-selected ions are guided via a second quadrupole ion guide into a temperature-controlled, He-filled octopole ion trap. The He pressure inside the trap is 0.1 mbar, which assures a sufficient amount of collisions ($\sim 5 \times 10^6$ s^{-1}) to thermalize the injected cluster anions to the ambient temperature. The trapped anions interact with the laser light. Light absorption can lead to photodetachment followed by photoionisation of the mass selected clusters. Positively charged ions are no longer confined along the axis of the octopole and are extracted from the trap. Clusters leaving the trap *via* the exit lens enter a second mass selecting quadrupole. The yield of mass-selected cations is measured by a subsequent off-axis conversion dynode detector.

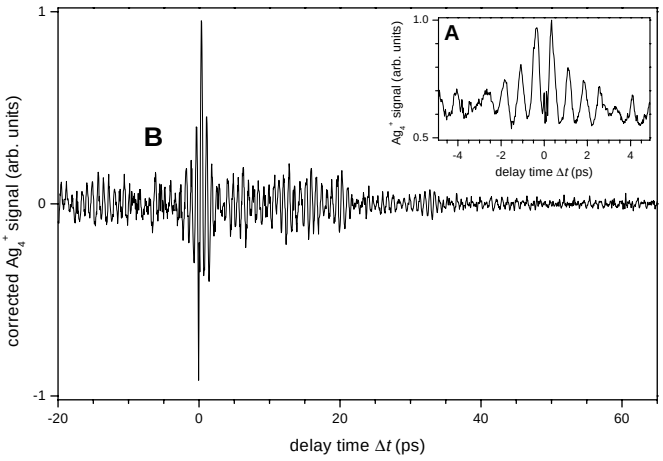

Fig. 1. One-color NeNePo spectra of Ag_4^- recorded at $\lambda_{max} =$ 385 nm and a mean anion temperature of 20 K. Trace A (top right) shows the uncorrected, mass selected Ag_4^+ yield. Trace B (center) is a composite of two measurements and the signal has been corrected for the following FFT analysis (see text).

3 Results

One-color ($h\nu_{pump} = h\nu_{probe}$) NeNePo spectra of Ag_4^- (432 amu) measured at $\lambda_{max} = 385$ nm and a mean anion temperature of 20 K are shown in Figure 1. Trace A (top right) shows the (uncorrected) mass selected Ag_4^+ yield as function of the delay time Δt between the pump and probe pulses from -4.9 ps to $+4.9$ ps in steps of 20 fs. The spectrum was normalized to the highest peak in the spectrum. $\Delta t = 0$ fs was calibrated using the well known NeNePo spectra of Ag_3^-. It can also be identified by the sharp interference pattern due to the temporal and spatial overlap of the two pulses. The pulse energy for both pulses was 7 μJ.

Trace B is a composite of two measurements covering delay times from -20 ps to $+20$ ps and $+20$ ps to $+65$ ps. These spectra were measured with pulse energies of 7 μJ for the pump pulse and 23 μJ for the probe pulse (at positive delay times). The spectra have been baseline corrected and transformed for the following fast Fourier transformation (FFT). This procedure has been described in detail elsewhere [31]. The raw spectra were normalized in such a way that the observed beat structure oscillates around zero. To this end a mean ion intensity averaged over 4 ps is determined and subtracted from the data set.

Trace A in Figure 1 shows a pronounced oscillatory structure, characterized by a period of $\sim$ 740 fs. The widths of the peaks are $\sim$ 290 fs. The intensity of the maxima decrease for larger values of $|\Delta t|$. Additional, weaker structures are observed at delay times > 2.8 ps overlapping the 740 fs beat structure. Note, that the oscillation in the signal intensity, which comprises up to 45 percent of the total signal, is superimposed on a constant signal background. The signal background stems from Ag_4^+ production by a single laser pulse. Because we focus the laser

beams into the center of the ion trap, the cross section for photodetachment followed by photoionization of the Ag_4 clusters is not negligible.

Trace B in Figure 1 shows oscillations in the corrected Ag_4^+ signal up to 60 ps, with decreasing intensity. Pronounced partial recurrences are observed at irregular intervals centered at 6, 12, 16, 20, 27 and 33 ps. At longer delay times oscillatory structure is still observed, but the decreasing signal-to-noise ratio makes a more detailed characterization of the structure increasingly difficult. Comparison of the data at positive delay times with the data at negative delay times shows a weak dependence on laser power. Positive delay times correspond to $E(h\nu_{pump}) = 7\ \mu$J and $E(h\nu_{probe}) = 23\ \mu$J and a roughly two times larger oscillatory signal is observed than for the reversed pulse sequence at negative time delays. More signal at positive delay times therefore indicates that an additional photon is required in the photoionization step compared to the photodetachment step.

The spectra in Figure 1 strongly resemble the pump-probe spectra of the related neutral alkali metal dimers and trimers measured in a molecular beam [31–33]. In these experiments pronounced oscillations in the ionization yield were interpreted in terms of vibrational wave packet dynamics. An ultrashort pump pulse generated a localized wave packet on an excited potential energy surface of the neutral. The wave packet motion was then probed by a second ultrafast pulse. The "location" of the wave packet could be characterized, due to a strong dependence of the ionization cross section on the normal coordinate of the involved vibrational mode(s), *i.e.*, on the relative position of the nuclei. Based on similar arguments we identify the main features in Figure 1 to result from vibrational wave packet dynamics on a potential energy surface of neutral Ag_4. A more detailed assignment will be discussed later. Assuming a single vibrational mode the roundtrip time of the wave packet is 740 ± 50 fs, yielding a mean vibrational frequency of 45 ± 4 cm^{-1}. We attribute the recurrences to effects of the anharmonicity of the potential, on which the wave packet propagates, resulting in dephasing and rephasing of the wave packet with time [34]. Complete recurrences are not observed. This is attributed to energy dissipative effects, mainly, IVR.

In order to characterize the main frequency components responsible for the oscillatory structure observed, the time domain spectrum was converted into the frequency domain using a standard fast Fourier transformation algorithm. In Figure 2 the FFT amplitude of trace B shown in Figure 1 is displayed as a function of energy. The dominant feature consists of several peaks centered around 45 cm^{-1}. At least eight peaks can be identified in the region from 32 to 60 cm^{-1}. Additional features are observed at 29 cm^{-1} (peak B) and at higher energies up to 100 cm^{-1}, in particular at 96 cm^{-1} (peak C).

Peaks A_1 to A_8 in Figure 2 are assigned to the difference in energy between adjacent vibrational levels of a single vibrational mode. If we denote the vibrational quantum number with v then this corresponds to the energy difference between levels with $\Delta v = \pm 1$. Assuming

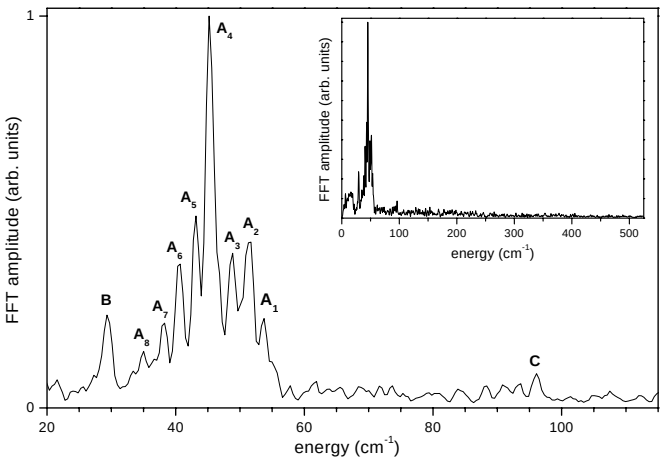

Fig. 2. Fast Fourier transform of trace B shown in Figure 1 for a spectral range from 20 cm^{-1} to 115 cm^{-1}, whereas the insert shows the same sequence in a range from 0 cm^{-1} to 520 cm^{-1}. The Fourier amplitude is plotted as a function of energy. See text for description of peak labels.

a Morse potential, for which the vibrational energy level spacings $\Delta G(v)$ are defined as

$$\Delta G(v) = \nu_0 \left[1 - 2\chi_e \left(v + 1\right)\right],$$

a linear least square fit yields an anharmonicity (slope) of $|2\nu_0\chi_e| = 2.65 \pm 0.05$ cm^{-1}. Determination of the anharmonicity constant is not straight forward, as no experimental evidence for the $v = 0$ level of this mode is available. The weak features observed in the region between 75 cm^{-1} to 100 cm^{-1}, *i.e.*, at roughly twice the mean frequency of 45 cm^{-1}, may then be assigned to vibrational energy level spacings with $\Delta G(v) = \pm 2$. The feature at 29 cm^{-1} (peak B) cannot be assigned.

4 Discussion

We now discuss the underlying energetics involved in the observed wave packet dynamics in neutral Ag_4. The anion photoelectron spectra of Ag_4^- show that three states of neutral Ag_4 are populated by a one photon process using 385 nm (3.22 eV) photons. These are the ^1A_g ground state and the $^3B_{1g}$ and $^1B_{1g}$ excited states of rhombic Ag_4 with vertical detachment energies of 1.65 eV, 2.39 eV, and 2.76 eV, respectively [17]. We thus narrow our following discussion to only involve these three states of neutral Ag_4. Multiphotonic photodetachment processes are in principle possible, but neglected in the following discussion due to their considerably smaller cross section compared to one-photon processes.

From each of the three mentioned states of neutral Ag_4 ionization into the rhombic $^2B_{3u}$ ground state of Ag_4^+ is allowed by a one-electron process [17]. The experimentally determined ionization energy of Ag_4 is 6.65 eV. Therefore

only the two excited states $^3B_{1g}$ and $^1B_{1g}$ may be ionized by a two photon process using 385 nm photons, while three 385 nm photons are required for ionization of the neutral ground state. Furthermore, the observation of oscillations in the NeNePo spectra require a dependence of the ionization cross section on the position of the nuclei, such that the ionization probability for one arrangement of the nuclei is considerably different from the ionization probability of another arrangement. In terms of wave packet dynamics these nuclear arrangements may be visualized as a wave packet, which is predominantly localized at either the inner or outer turning point of the PES it is propagating on. Thus the photoionization energy should be in the vicinity of the vertical ionization potential. This holds for $^3B_{1g}$ and $^1B_{1g}$ states but not the ^1A_g ground state.

Ab initio calculations on the harmonic frequencies of the low-lying electronic states of rhombic Ag_4 clearly favor the excited states $^3B_{1g}$ and $^1B_{1g}$ over the ^1A_g state to be involved in the observed wave packet dynamics [35]. In general, only totally symmetric modes of the neutral cluster may be directly excited upon photodetachment. Among the six normal modes of rhombic Ag_4, only two of them, both in-plane ring-breathing modes, have a_g symmetry. The calculated frequencies for the $1a_g$ mode are 196 cm^{-1} (^1A_g), 144 cm^{-1} ($^3B_{1g}$) and 142 cm^{-1} ($^1B_{1g}$). The calculated frequencies for the $2a_g$ mode are 114 cm^{-1} (^1A_g), 53 cm^{-1} ($^3B_{1g}$) and 50 cm^{-1} ($^1B_{1g}$). Reasonable agreement with the present experiment (45 cm^{-1}) is only found for the $2a_g$ mode of either the $^3B_{1g}$ or $^1B_{1g}$ electronically excited state of Ag_4. These calculations also confirm the pronounced anharmonicity of this vibrational mode.

We conclude that the oscillations observed in the NeNePo spectra of Ag_4 are due to vibrational wave packet dynamics in the $2a_g$ mode of either the $^3B_{1g}$ or $^1B_{1g}$ 'dark' electronically excited state of rhombic Ag_4. A localized wave packet is created on the electronically excited PES of neutral Ag_4 by one-photon detachment of Ag_4^- in its electronic ground state. The wave packet motion is then probed by a two-photon photoionization step to the ground state of Ag_4^+. The $2a_g$ mode was not resolved in the previous anion photoelectron spectroscopy studies, due to its low frequency of 45 cm^{-1}, which lies below the energy resolution ($\geq$ 80 cm^{-1}) of conventional anion photoelectron spectrometers.

The present results demonstrate the first successful application of femtosecond NeNePo spectroscopy to study the wave packet dynamics, manifested by a beat structure in the cation yield, in real time in a "purely" bound potential, in contrast to the previous transition-state experiments on the silver trimer which connected linear with triangular structures. The spectra enable us to precisely characterize a selected vibrational mode with a resolution, which is superior to that of conventional frequency domain techniques that have been applied to the study of the silver tetramer. We are planning to extend these studies and access the vibrational wave packet dynamics in the ground state of Ag_4. Experimental modifications necessary for this experiment are currently in progress in our laboratory and when finished they will enable us to use shorter pulses (40 fs) and continuously tune the pulse wave length in the region from 250 nm to 2600 nm.

The authors wish to express their thanks to V. Bonačić-Koutecký, M. Hartmann, and R. Mitrić for providing us with their results prior to publication and for helpful discussions. K.R.A. gratefully acknowledges a stipend from the Swiss National Science Foundation. The research was supported by the Deutsche Forschungsgesellschaft as part of the SFB 450 and SFB 546.

References

1. *Ultrafast Phenomena XII*, edited by T. Elsaesser, S. Mukamel, M. Murnane, N.F. Scherer (Springer, Berlin, 2000), Vol. 66.
2. A. Zewail, J. Phys. Chem. A **104**, 5660 (2000).
3. *Femtosecond Chemistry*, edited by J. Manz, L. Wöste (VCH, Weinheim, 1995).
4. S. Wolf, G. Sommerer, S. Rutz, E. Schreiber, T. Leisner, L. Wöste, Phys. Rev Lett. **74**, 4177 (1995).
5. D.W. Boo, Y. Ozaki, L.H. Anderson, W.C. Lineberger, J. Phys. Chem. A **101**, 6688 (1997).
6. S. Wolf, Ph.D. thesis, Freie Universität Berlin, Berlin, 1997.
7. T. Leisner, S. Vajda, S. Wolf, L. Wöste, R.S. Berry, J. Chem. Phys. **111**, 1017 (1999).
8. H. Hess, S. Kwiet, L. Socaciu, S. Wolf, T. Leisner, L. Wöste, Appl. Phys. B **71**, 337 (2000).
9. H.O. Jeschke, M.E. Garcia, K.H. Bennemann, Phys. Rev. A **54**, R4601 (1996).
10. M. Hartmann, J. Pittner, V. Bonačić-Koutecký, A. Heidenreich, J. Jortner, J. Chem. Phys. **108**, 3096 (1998).
11. M. Hartmann, A. Heidenreich, J. Pittner, V. Bonačić-Koutecký, J. Jortner, J. Phys. Chem. A **102**, 4069 (1998).
12. I. Andrianov, V. Bonačić-Koutecký, M. Hartmann, J. Manz, J. Pittner, K. Sundermann, Chem. Phys. Lett. **318**, 256 (2000).
13. T. Leisner, S. Rutz, G. Sommerer, S. Vajda, S. Wolf, E. Schreiber, L. Wöste, in *Fast Elementary Processes in Chemical and Biological Systems*, edited by A. Tramer (AIP Press, Woodbury, New York, 1996), pp. 603-609.
14. M. Warken, V. Bonačić-Koutecký, Chem. Phys. Lett. **272**, 284 (1997).
15. C. Yannouleas, U. Landman, J. Phys. Chem. A **102**, 2505 (1998).
16. G. Ganteför, M. Gausa, K.-H. Meiwes-Broer, H.O. Lutz, J. Chem. Soc. Faraday Trans. **86**, 2483 (1990).
17. J. Ho, K.M. Ervin, W.C. Lineberger, J. Chem. Phys. **93**, 6987 (1990).
18. H. Handschuh, C.-Y. Cha, H. Möller, P.S. Bechthold, G. Ganteför, W. Eberhardt, Chem. Phys. Lett. **227**, 496 (1994).
19. H. Handschuh, C.-Y. Cha, P.S. Bechthold, G. Ganteför, W. Eberhardt, J. Chem. Phys. **102**, 6406 (1995).
20. K.J. Taylor, C.L. Pettiette-Hall, O. Cheshnovsky, R.E. Smalley, J. Chem. Phys. **96**, 3319 (1992).
21. C. Félix, C. Sieber, W. Harbich, J. Buttet, I. Rabin, W. Schulze, G. Ertl, Chem. Phys. Lett. **313**, 105 (1999).
22. P.R. Taylor, J.M.L. Martin, J.P. Francois, R. Gijbels, J. Phys. Chem. **95**, 6530 (1991).

23. C. Jackschath, I. Rabin, W. Schulze, Z. Phys. D **22**, 517 (1992).
24. V. Bonačić-Koutecký, L. Češpiva, P. Fantucci, J. Pittner, J. Koutecký, J. Chem. Phys. **98**, 7981 (1993).
25. V. Bonačić-Koutecký, L. Češpiva, P. Fantucci, J. Pittner, J. Koutecký, J. Chem. Phys. **100**, 490 (1994).
26. R. Santamaria, I.G. Kaplan, O. Novaro, Chem. Phys. Lett. **218**, 395 (1994).
27. V. Bonačić-Koutecký, J. Pittner, M. Boiron, P. Fantucci, J. Chem. Phys. **110**, 3876 (1999).
28. Z.F. Liu, W.L. Yim, J.S. Tse, J. Hafner, Eur. Phys. J. D **10**, 105 (2000).
29. U. Heiz, W.-D. Schneider, J. Phys. D **33**, R85 (2000).
30. P. Fayet, F. Granzer, G. Hegenbart, E. Moisar, B. Pishel, L. Wöste, Phys. Rev. Lett. **55**, 3002 (1985).
31. S. Rutz, Ph.D. thesis, Freie Universität Berlin, Berlin, 1996.
32. T. Baumert, M. Grosser, R. Thalweiser, G. Gerber, Phys. Rev. Lett. **67**, 3753 (1991).
33. S. Rutz, K. Kobe, H. Kuhling, E. Schreiber, L. Wöste, Z. Phys. D **26**, 276 (1993).
34. M. Gruebele, A.H. Zewail, J. Chem. Phys. **98**, 883 (1993).
35. M. Hartmann, V. Bonačić-Koutecký, private communication (2000).